

Investigation of the log region structure in wall bounded turbulence*

Nicholas Hutchins[†] and Ivan Marusic[‡]

Aerospace Engineering and Mechanics, University of Minnesota, Minneapolis, MN 55455, USA

Multiple plane stereo PIV results and data from a rake of ten hot-wire probes are used to investigate the largest scale structures in the logarithmic region of a zero-pressure-gradient turbulent boundary layer. Studies over the past few years have reported that wall-parallel plane PIV vector fields are dominated by long meandering stripes of positive and negative u fluctuation. Such features alternate in the spanwise direction and carry a large proportion of the Reynolds shear stress in the outer regions [7, 21]. The size of these features appears to scale well with outer variables. A pronounced vortical structure is noted clustered about the elongated regions of momentum deficit in arrangements that have previously been termed hairpin packets [2, 7, 8, 11, 17, 21]. Since the PIV fails to adequately capture the full streamwise extent of the low-speed regions, a rake of hot-wire probes is also employed to capture a continuous view of the spanwise coherence. These complementary measurements reveal that the structures can be extremely long in the streamwise direction (often exceeding 20δ in length). These large-scale structures maintain a presence in the near-wall region, imposing low wave-number energy on to the buffer region.

I. Introduction

The first part of this paper reviews the results from a series of multiple-plane stereo PIV measurements conducted at the University of Minnesota over the past few years. These results show clear evidence that the log (or overlap) region of the turbulent boundary layer has a dominate feature of long meandering stripes of positive and negative u fluctuation. Much of these results are reported in a chapter by Marusic and Hutchins[17]. These large structures are further investigated by analyzing time-series data from a rake of 10 hot-wires, and full three-dimensional data from a DNS dataset.

II. PIV data

Figure 1 shows example u fluctuations from recent combined plane PIV measurements, whereby stereoscopic views of the streamwise / spanwise and streamwise / wall-normal plane are simultaneously acquired (see [8] for experimental details). Throughout this paper, the axis system x, y and z refer to the streamwise, spanwise and wall-normal directions, with u, v and w describing the respective fluctuating velocity components. In all cases gray shading shows negative streamwise velocity fluctuations (positive fluctuations are set to white). Together these plots illustrate some of the recognized emergent features in the log region. The horizontal plane of Figure 1 (a) clearly exhibits the spanwise stripiness noted by [7] and [21]. Elongated low-momentum regions persist for the entire streamwise length of the viewing window, with signs of spanwise repetition. The simultaneous side view of plot (b) demonstrates that these features have a wider three-dimensional structure, extending some considerable distance in the wall-normal direction. In all cited cases high momentum fluid has been noted to fill the regions between the low momentum stripes. Together

*Copyright © by Nicholas Hutchins and Ivan Marusic. Published by AIAA Inc., with permission.

[†]Postdoctoral Associate

[‡]Associate Professor, AIAA member

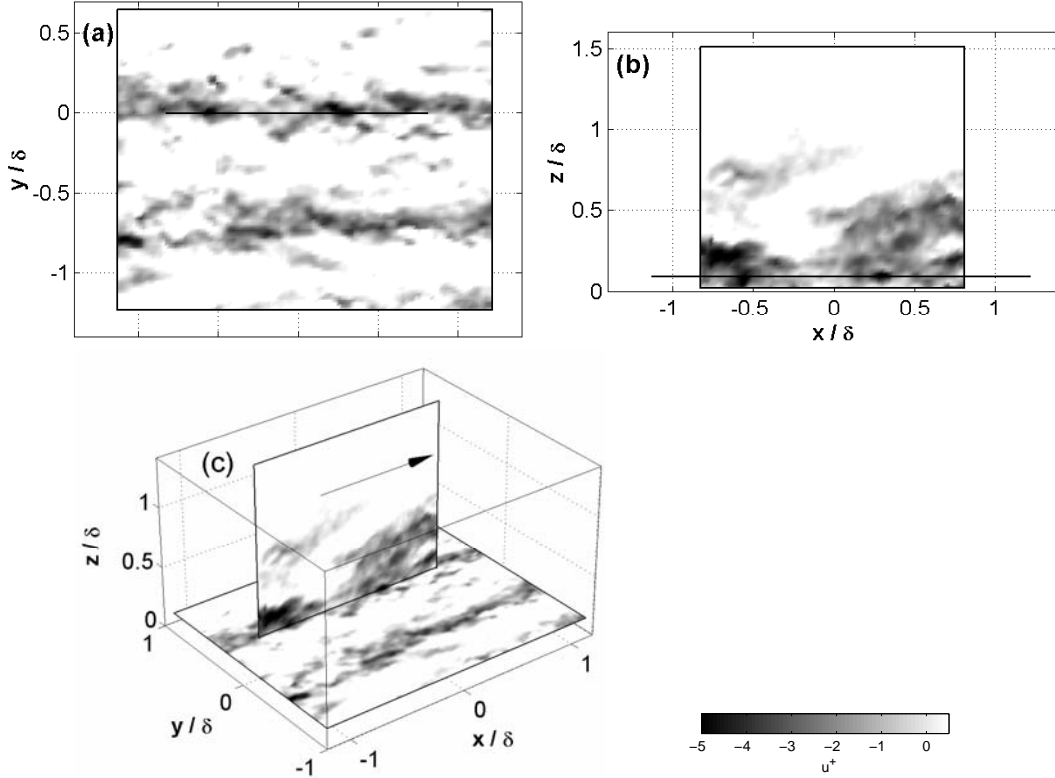


Figure 1. Example instantaneous negative u fluctuations from the combined-plane PIV. (a) plan-view showing horizontal plane; (b) side-view showing vertical plane; (c) orthogonal projection showing both planes. Thick horizontal lines on plots (a & b) show plane intersects. Gray shading shows negative u fluctuations (see key).

these features dominate the two-point correlations of the streamwise velocity fluctuations (R_{uu}) throughout the log region. Figure 2 shows iso-contours of R_{uu} at $z/\delta = 0.087$ calculated from various PIV planes (see [11] for details of the inclined plane experiments). Elongated positive correlation regions are flanked in the spanwise direction by anti-correlated behavior (dashed contours), clearly reflecting the spanwise stripiness of high- and low-momentum regions previously noted of Figure 1. It is clear from Figure 2 (d) and from the 45° and 135° comparison of plots (b & c) that the correlated regions are inclined in the downstream direction.

The resolved large-scale u fluctuations are associated with a wider (and more complex) vortical structure. Here we use the two-dimensional swirl approximation λ_{ci} as an identifier of vortex cores, as described in [1, 2]. Figure 3 shows the streamwise velocity fluctuations with signed swirl in an example combined-plane experiment result. The frame is selected such that an elongated low momentum streak lies on the intersection of the vertical and horizontal planes. Plots (b) and (d) show the fluctuating streamwise velocity in the two orthogonal planes. Figure 3(c) shows the associated magnitude of the signed swirl λ_s (signed swirl is obtained by multiplying λ_{ci} with the sign of the local out-of-plane vorticity component). In the absence of vortical activity, swirl is everywhere zero. Red shaded patches show regions of positive signed swirl (counter-clockwise), while the blue areas indicate negative rotation (clockwise). Careful inspection of the figure shows a clear correlation between the patches of signed swirl and the superimposed negative u fluctuation regions (shown as gray shaded regions in c & e). The swirl events of Figure 3(c) are seen to be strongly associated with the flanks of the low-speed regions (the patches are predominantly arranged on the contours). Furthermore, the patches are arranged such that positive swirls tend to be situated on the $-y$ flank of the low-speed region, whilst negative swirls tend to align on the $+y$ side. Two-dimensional swirl essentially marks vortex cores that have pierced the measurement plane (at some oblique angle). The implication from

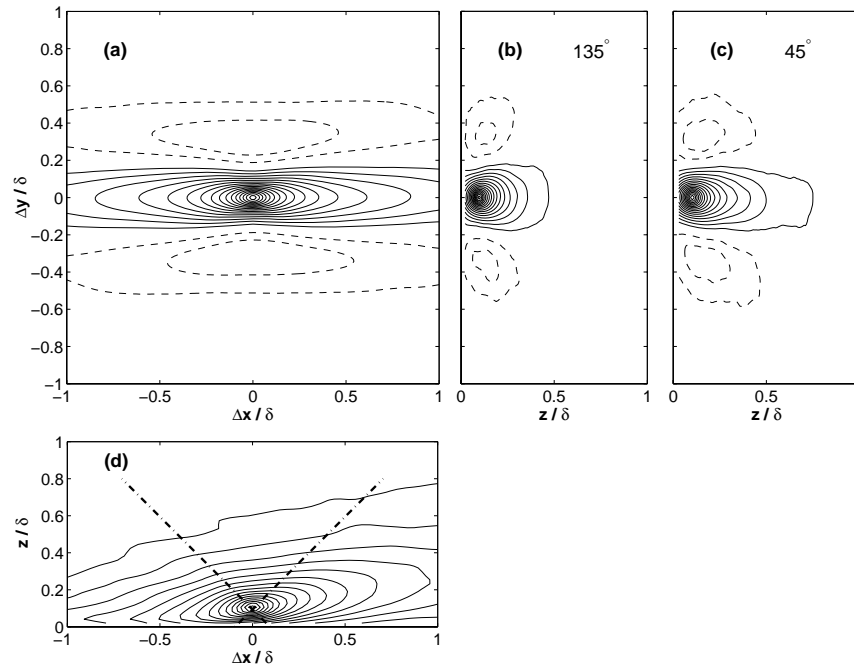


Figure 2. Two-point correlations of the streamwise velocity fluctuation R_{uu} calculated at $z_{ref}/\delta = 0.087$ for (a) wall-parallel plane from combined plane; (b) 135° inclined plane; (c) 45° inclined plane; (d) vertical-plane from combined experiments. Contour levels are from $R_{uu} = -0.12$ to 0.96 in increments of 0.06 . Solid lines show positive contours and dashed show negative.

Figure 3(c), is that the previously observed large-scale stripes are associated with complex (yet quite well-defined) arrangements of smaller-scale vortical structures. Such arrangements have been previously reported for wall-parallel plane measurements [21, 7]. Figure 3(d) shows the simultaneous velocity fluctuations in the vertical plane. The corresponding swirl pattern is shown on Figure 3(e). In this view almost all of the swirl is positive, which of course reflects the mean spanwise vorticity due to the shear layer (in side-view, positive swirl is indicative of clockwise rotation, since the y axis acts into the page). These swirl patches mark vortex cores that are primarily spanwise aligned. Though the structure is clearly complex, we again see signs that vortex cores are aligned along the edge of low-speed regions. There appears to be an array of spanwise vortices arranged along the inclined back of the previously observed low-momentum region.

The observed arrangements of vortices about negative u fluctuations (as noted in Figure 3) can be largely explained by the hairpin packet paradigm [2]. Figure 4 shows sketches of an idealized hairpin packet along with representations of the light-sheet orientations used in the combined-plane experiments (light-sheets are shown as green planes). Darker green shading in the interior of the packet structure shows regions of predicted negative u fluctuation (this is due to a mutual backwards flow induced by the hairpin vortices). Regions where positive and negative two-dimensional swirl occur are colored red and blue respectively (i.e. regions where the measurement plane makes an approximately perpendicular cut through a vortex core). For both cases, the shape of the low-momentum regions and the arrangements of the swirl patches about these, match the observations from the instantaneous examples shown in Figure 3. In the wall-parallel plane (Figure 4a), the packet structure imposes an elongated low-speed streak onto the measurement plane. The cut made through the necks of the vortices will lead to a series of positive signed swirls aligned on the $-y$ side of the streak (with negative signed vortices populating the opposite flank). This is the pattern observed in Figure 3. For the vertical plane (Figure 4b), the packet signature will be an inclined low-speed region with positive signed swirl events aligned along the inclined back. In this plane there is no negative signed swirl attributed to the packet structure. This matches closely the observations from Figures 3(d & e).

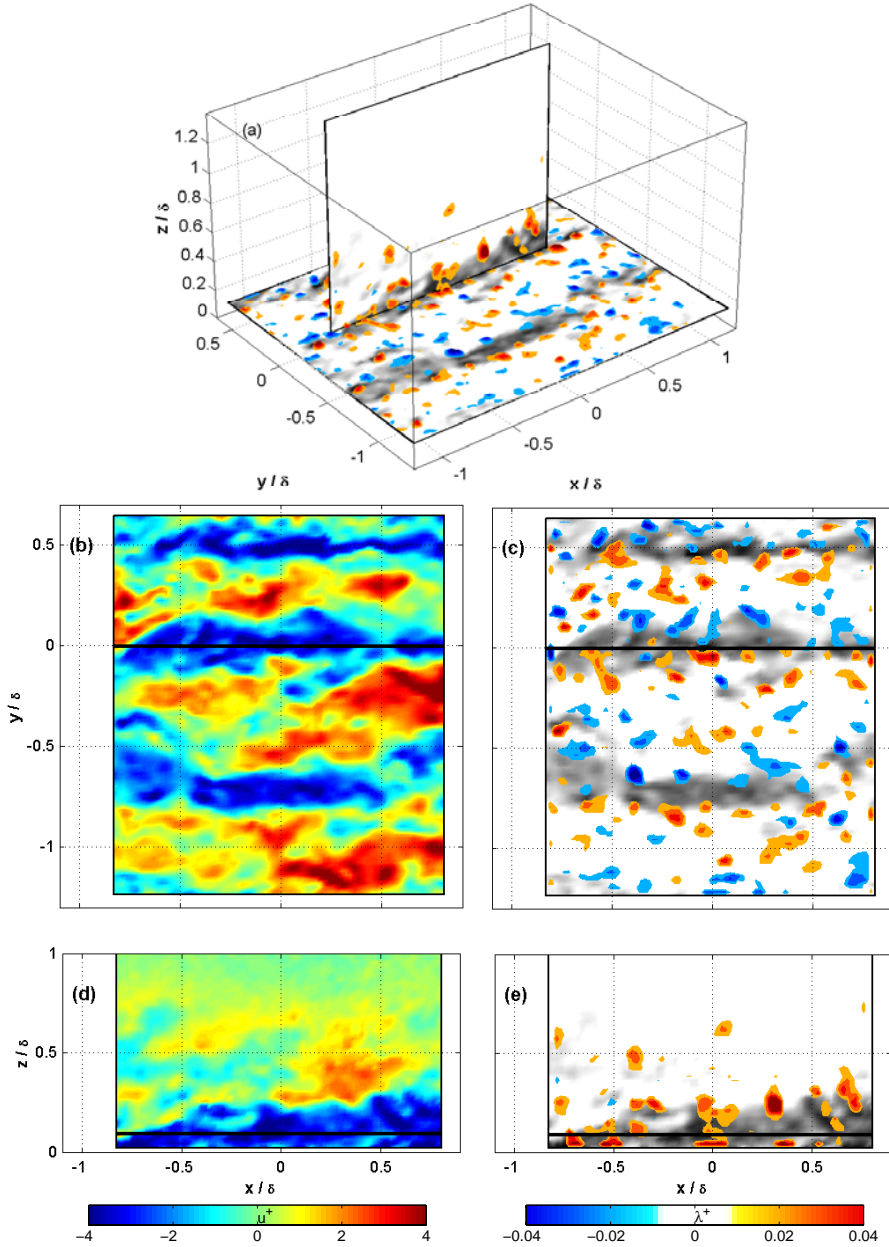


Figure 3. (a) Three-dimensional view of both orthogonal planes, (b, c) plan-view of horizontal plane and (d, e) side-view of vertical plane for example instantaneous flow-field. Plots (b,e) show streamwise velocity fluctuation as color shading. Plots (a, b, d) show instantaneous signed swirl (color scale indicates fluctuation magnitude) with gray-scale contours of streamwise velocity fluctuation superimposed (gray-scale as Figure 1).

It has been shown that a considerable proportion of the Reynolds shear stress in the log and wake region is associated with the large-scale features under discussion here [7]. Figure 5 shows the wall-normal and Reynolds shear stress fluctuations for the example combined-plane frame-set originally studied in Figure 3. The left-hand plots show the wall-normal velocity fluctuations. Only the positive w fluctuations are shown (shaded gray) with contours of negative u fluctuation superimposed over the top (at $u^+ = -1$). Clearly, the elongated low-speed regions are predominantly characterized by positive wall-normal fluctuations. These ejection events are strong positive contributors to Reynolds shear stress. This is confirmed by the right-hand

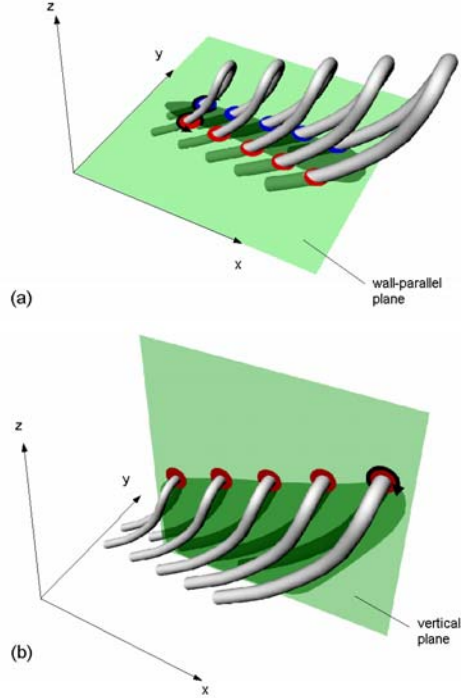


Figure 4. Idealized packet of inclined hairpin eddies imaged by (a) wall-parallel light-sheet; (b) vertical (streamwise-spanwise) light-sheet; • Red patches show positive swirl. • Blue patches show negative. Darker green shadow on light-sheet indicates predicted region of negative u fluctuation.

plots (b & d) which show the fluctuating Reynolds shear stress ($-uw$) for the horizontal and vertical planes respectively. The localized concentrations of $-uw$ primarily occupy the interior of the low-speed contour. These patches of Reynolds shear stress concentration are highly localized. This is presumably because the Q2 and Q4 events are associated with individual vortex cores that are themselves clustered about the long low-speed regions. Certainly a comparison of Figures 3 and 5 would support this scenario, with Reynolds stress concentrations tending to coincide with nearby swirl events. This spatial compactness is reflected in single point statistics such as the energy spectra of the Reynolds shear stress fluctuations. However, the important point that could be missed from such statistics is that, though the Reynolds stress fluctuation itself does not contain energy at very low wave-numbers, the individual spatially compact concentrations exhibit a strong alignment with the largest u modes (and it is shown below that these modes can be extraordinarily long in the streamwise direction).

III. Hot-wire rake results

For the instantaneous flow-fields and the correlation maps shown above, the length of the log-region structures has exceeded the PIV field-of-view. There is some evidence in the literature that these features can attain very large streamwise dimensions in pipes, channel flows and atmospheric surface layers. Hot-film measurements in pipe flows seem to show that streamwise energetic modes can extend up to 12-14 pipe radii [16]. More recent analysis of large numerical domain DNS results (in particular 2D spectra) have shown that in the log region, Φ_{uu} energy can reside in very long streamwise modes for larger k_y bands (certainly > 20 channel half heights, see [4, 13]). Large streak-like features have also been noted in the atmospheric surface layer, both in experiment and LES studies (up to several kilometers in length, see [6]).

In light of these suggested length-scales, and in recognition of the limited fields of view afforded by PIV, a spanwise rake of 10 hot-wire sensors has been used to capture the true extent of the largest scales. The idea is to use the fluctuating signals from the ten hot-wire probes to reconstruct the instantaneous

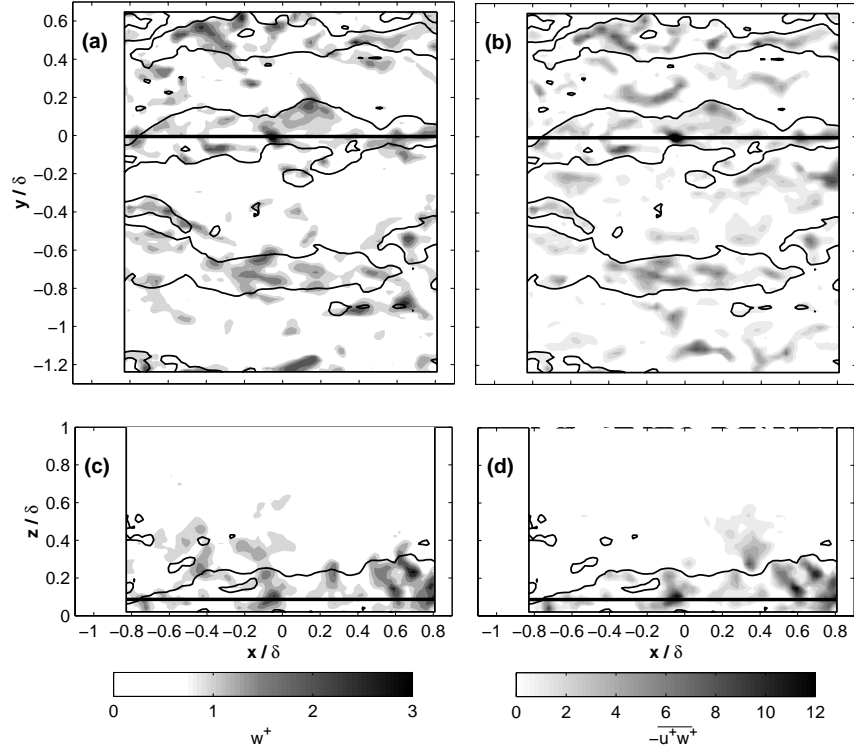


Figure 5. Example frame-set from combined plane experiment. Left-hand plots show positive wall-normal velocity fluctuations in (a) the horizontal and (c) the vertical planes. Gray shading shows $w > 0.5U_\tau$ (see color scale). Right-hand side shows Reynolds shear stress for (b) horizontal and (d) vertical planes. Gray shading shows $-\overline{u^+w^+} > 0$ (see color scale). Solid contours show negative u fluctuations ($u^+ = -1$).

spanwise profile of the u velocity fluctuation. By projecting this signal in time and using Taylor’s hypothesis (frozen convection) a view of the long high- and low-speed streaks can be constructed that covers a much larger streamwise domain than that available with PIV. Rake measurements were performed in two separate facilities covering a wide range of Reynolds numbers (from $Re_\tau = 1120$ to 19960). Full experimental details are given in [12].

Figure 6 shows the outer-scaled two-point correlation of streamwise velocity fluctuation (R_{uu}) for the rake experiments. The left-hand-side shows the correlations in the streamwise direction at $\Delta y = 0$. This is the autocorrelation, or the streamwise slice at $\Delta y = 0$ through a correlation map of the type shown in Figure 2(a). The right-hand-side shows the spanwise variation of R_{uu} . For all available Reynolds numbers, spanning well over a decade in Re_τ , there is a good collapse in the outer-scaled R_{uu} . This is all the more striking given the large variation in δ across the experiments (from 0.069 to 0.336 mm). Outer-scaling of correlation contours in the log and wake regions has also been observed by [19], [22] and [11]. The correlation profiles from inclined plane PIV of [11] are included for comparison on the right-hand plots of Figure 6.

Comparing the plots in Figure 6 from top to bottom, reveals that the length of the correlations increases throughout the log region (up to $z/\delta = 0.15$), with a pronounced shortening occurring in the upper wake region ($z/\delta = 0.50$). The spanwise width of the correlation region increases approximately linearly with z/δ for all heights investigated (noted for inclined-plane PIV by [11]).

The streamwise extent of the log region structures has been previously inferred from single-point statistics such as those shown on the left-hand-side of Figure 6. For turbulent boundary layers, the long-tails in the autocorrelation curves (the extent of the positive R_{uu} region on the left-hand plots of Figure 6) and the peak in the pre-multiplied spectra $k_x\Phi_{uu}$ have consistently indicated length-scales $O(6\delta)$. In reality, when raw

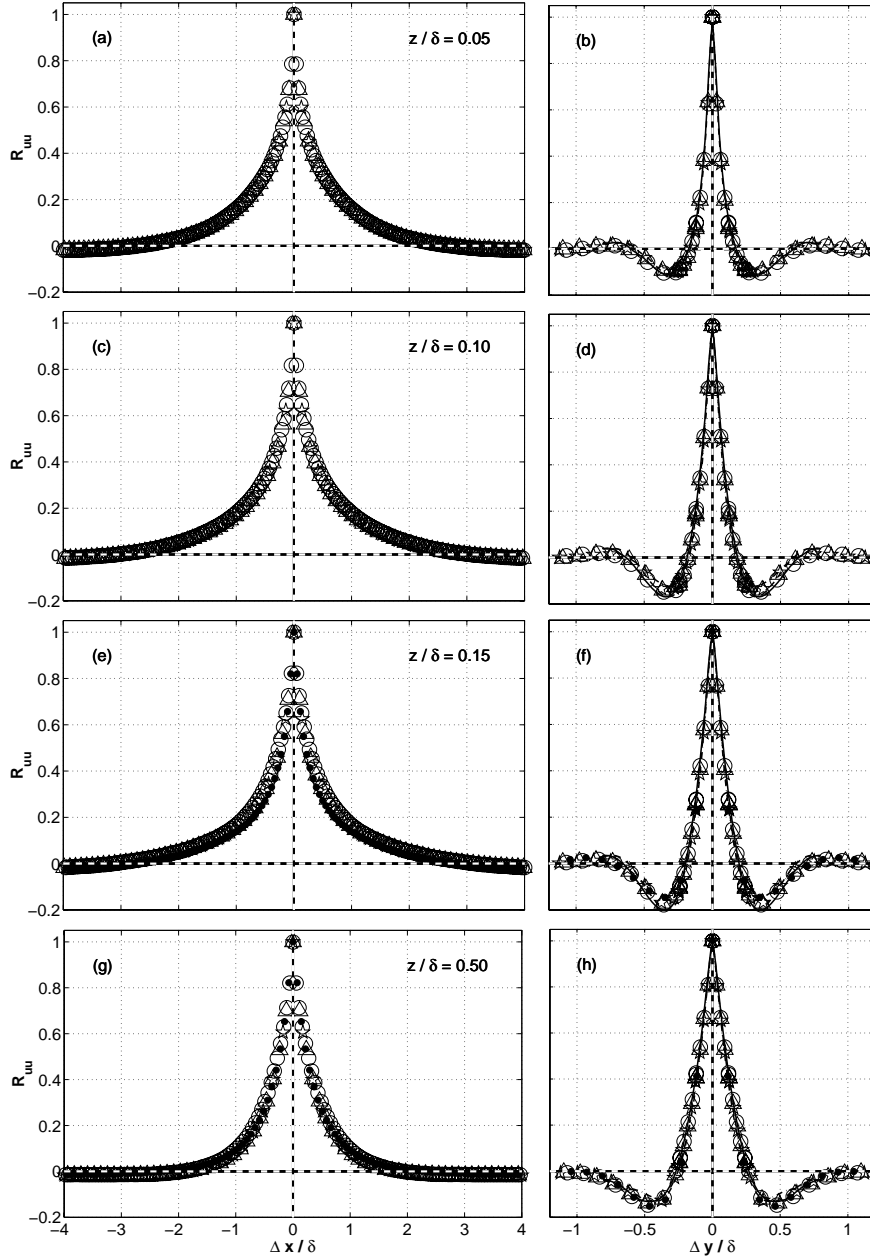


Figure 6. Streamwise (left) and spanwise (right) two-point correlations of the streamwise velocity fluctuation R_{uu} calculated at (a, b) $z_{ref}/\delta = 0.05$; (c, d) $z_{ref}/\delta = 0.10$; (e, f) $z_{ref}/\delta = 0.15$; (g, h) $z_{ref}/\delta = 0.10$. Symbols show rake data (\bullet) $Re_\tau = 1120$; (\circ) $Re_\tau = 7610$; (\triangle) $Re_\tau = 14380$; (\star) $Re_\tau = 19960$. Lines show 45° inclined plane PIV results (dash-dot) $Re_\tau = 1010$; (dashed) $Re_\tau = 1840$; (solid) $Re_\tau = 2800$.

fluctuating velocity signals from the rake are viewed, we commonly see features that are far in excess of these length-scales. Figure 7(a) shows an example segment from the rake at $z/\delta = 0.15$. A very long meandering feature appears to snake through the measurement domain for over 20δ . For the Reynolds number shown ($Re_\tau = 14380$) this amounts to a physical length of over 6.5 m. This implies that the log region stripiness previously observed from PIV data is actually a snapshot of a far larger structure (see the PIV comparison of plot b). Furthermore, although the low-speed region in Figure 7(a) is clearly very long, the meandering tendency will mask its true length from single point statistics.

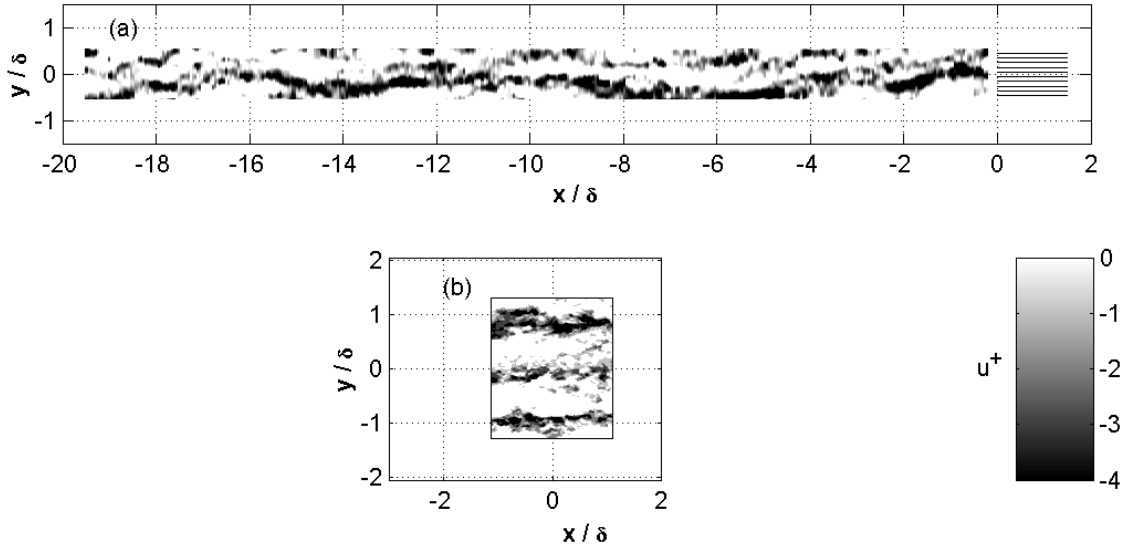


Figure 7. (a) Example rake signal at $z/\delta = 0.15$ for $Re_\tau = 14380$. x -axis is reconstructed using Taylor's hypothesis and a convection velocity based on the local mean, $\bar{U} = 15.9 \text{ ms}^{-1}$. (b) Typical PIV frame for comparison. Shading shows only negative u fluctuations (see gray-scale).

This point is clarified in [9, 12] through the study of a synthetic flow composed only of sinusoidally meandering low- and high-speed regions. As well as demonstrating how spanwise wandering can shorten the length-scale inferred from single point statistics, this simple model also successfully recreates the distinctive patterns noted in the far-field behavior of the two-point correlations R_{uu} (principally the tendency for negative R_{uu} values noted for $x/\delta > \pm 3$ in the left-hand plots of Figure 6).

IV. Evidence from direct numerical simulations

The advent of large numerical domain DNS has also uncovered evidence of these largest scales. Figure 8 shows streamwise velocity fluctuations from recent channel flow simulations at $Re_\tau = 950$ [5]. Plot (a) shows the negative u fluctuations in the log region ($z^+ = 150$), and also for the corresponding field in the viscous buffer zone ($z^+ = 15$) at the wall-normal location of maximum turbulent energy production. Clearly the numerical simulations exhibit a similar spanwise stripiness in the u fluctuations, with evidence of very long streamwise features and spanwise wandering for the log region. For the $z^+ = 15$ plane, inner-scaled streaks are seen to dominate with streamwise and spanwise lengthscales $\lambda_x^+ \approx 1000$ and $\lambda_z^+ \approx 100$ commonly reported (e.g. [14]). If we peer through the small inner-scaled structures at $z^+ = 15$, we can see a faint superimposed footprint of the larger-scale features. This is made clear in figure 8(b) which shows the same results but with a low-pass filter of length scale δ applied to highlight only the large scale structures. Plotted in this manner, the coupling between the large structures is much more obvious. It has been shown previously that the large-scale log and wake region events retain a measurable correlation with the near-wall buffer region ('attached' and 'detached' correlation regimes [11]). By such mechanisms very low wave-number energy leaches into the near-wall region. By highlighting the superposition of these two different scales, Figure 8 offers a very clear example of the Reynolds number dependence of the streamwise energy in the sub-layer and buffer region that has been noted in other studies in the past few years (for example [15, 20, 3, 18]).

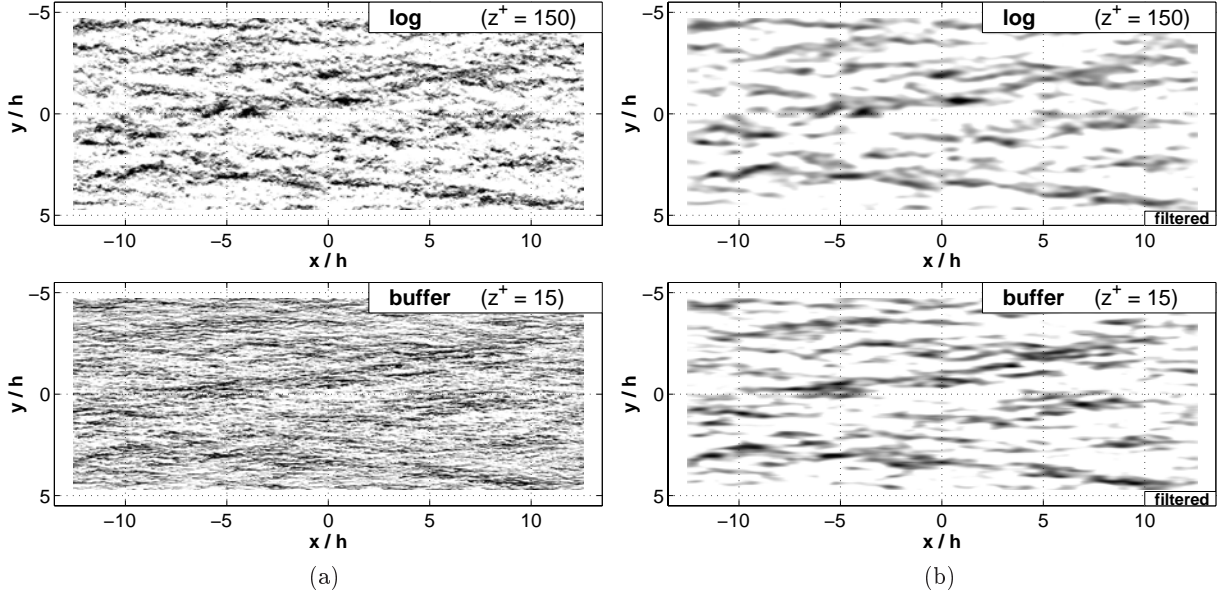


Figure 8. Grayscale contours of negative streamwise velocity fluctuation for two streamwise-spanwise planes at $z^+ = 150$ (nominally in log layer) and at $z^+ = 15$ (in near-wall viscous buffer region). DNS channel data, $Re_\tau = 950$. Gaussian filtered plots highlight large scale structures ($> O(\delta)$). Note “footprint” of large-scale structures from $z^+ = 150$ plane in the $z^+ = 15$ plane.

V. Concluding remarks

Multi-plane stereoscopic PIV, hot-wire rake measurements, and DNS data provide good insights into the characterization of the larger-scale coherent structure in the logarithmic and wake regions of a turbulent boundary layer. The results show consistent evidence of large streamwise structures in the log region characterized by a pronounced spanwise stripiness of alternating high- and low-momentum, with such stripiness in u extending a considerable distance in the wall-normal direction. These structures appear to be very long in the streamwise direction, with spanwise meandering tending to mask their true lengths in one-point measurements. An associated vortical structure is noted with multiple swirling motions appearing to be clustered around the stripes of momentum deficit. The precise arrangement and sign of these associated swirl patches, would suggest that the hairpin packet paradigm provides a good descriptive kinematic model for this clustering. Further work is required to understand the origin and mechanisms responsible for these large structures.

The large structures are also found to scale with outer variables, and impose low wave-number energy onto the viscous buffer region. This is consistent with mixed (inner and outer) scaling for the streamwise (and spanwise) turbulence intensities. The presence of the wall (blocking or the associated “image vortex structures” in the wall) prevent this mixed scaling for the wall-normal turbulence intensity or Reynolds shear stress.

As a final comment, the observed “superstructures” would seem to be viable targets for control schemes. This is particularly the case given that they are very large and carry so much of the Reynolds stress in the log region, while maintaining an apparent dynamic link with the near-wall region. Though they are perhaps not so amenable to wall based actuation, these structures do have the advantage that they are very large, scale on boundary layer thickness, and also seem to obey preferred spanwise spacing modes [10]. Thus for higher Reynolds numbers, they might provide a more realistic target for active control schemes based on large-scale manipulation. In the interim it would certainly be interesting to study the passive modification of these structures.

Acknowledgments

The authors gratefully acknowledge support from the National Science Foundation (Grant CTS 0324898) and the David and Lucile Packard Foundation. The majority of the experimental work was undertaken jointly with B. Ganapathisubramani and W. Hambleton. The authors also thank Professor R. D. Moser for kindly making the $Re_\tau = 950$ DNS data available, and Professor M. S. Chong for hosting the Melbourne experiments.

References

- ¹ R. J. Adrian, K. T. Christensen, and Z.-C. Lui. Analysis and interpretation of instantaneous turbulent velocity fields. *Exp. Fluids*, 29:275–290, 2000.
- ² R. J. Adrian, C. D. Meinhart, and C. D. Tomkins. Vortex organization in the outer region of the turbulent boundary layer. *J. Fluid Mech.*, 422:1–54, 2000.
- ³ D. B. DeGraaff and J. K. Eaton. Reynolds number scaling of the flat-plate turbulent boundary layer. *J. Fluid Mech.*, 422:319–346, 2000.
- ⁴ J. C. del Álamo and J. Jiménez. Spectra of the very large anisotropic scales in turbulent channels. *Phys. Fluids*, 15:41–44, 2003.
- ⁵ J. C. del Álamo, J. Jiménez, P. Zandonade, and R. D. Moser. Scaling of the energy spectra of turbulent channels. *J. Fluid Mech.*, 500:135–144, 2004.
- ⁶ P. Drobinski, P. Carlotti, R. K. Newsom, R. M. Banta, R. C. Foster, and J.-L. Redelsperger. The structure of the near-neutral atmospheric surface layer. *J. Atmos. Sci.*, 61:699–714, 2004.
- ⁷ B. Ganapathisubramani, E. K. Longmire, and I. Marusic. Characteristics of vortex packets in turbulent boundary layers. *J. Fluid Mech.*, 478:35–46, 2003.
- ⁸ W. T. Hambleton, N. Hutchins, and I. Marusic. Multiple plane PIV measurements in a turbulent boundary layer. *J. Fluid Mech.*, 2005. In press.
- ⁹ N. Hutchins, B. Ganapathisubramani, and I. Marusic. Dominant spanwise Fourier modes, and the existence of very large scale coherence in turbulent boundary layers. In M. Behnia, W. Lin, and G. D. McBain, editors, *Proceedings of the 15th Australasian Fluid Mechanics Conference*, 2004.
- ¹⁰ N. Hutchins, B. Ganapathisubramani, and I. Marusic. Spanwise periodicity and the existence of very large scale coherence in turbulent boundary layers. In *Proceedings of the the Fourth International Symposium on Turbulence and Shear Flow Phenomena*, 2005.
- ¹¹ N. Hutchins, W. T. Hambleton, and I. Marusic. Inclined cross-stream stereo PIV measurements in turbulent boundary layers. *J. Fluid Mech.*, 541:21–54, 2005.
- ¹² N. Hutchins and I. Marusic. Evidence of very long meandering streamwise structures in the logarithmic region of turbulent boundary layers. *J. Fluid Mech.*, 2005. Under review.
- ¹³ J. Jiménez. The largest scales of turbulent wall flows. In *CTR Annual Research Briefs*, Progress in Astronautics and Aeronautics, pages 943–945. Stanford University, 1998.
- ¹⁴ J. Jiménez and J. C. del Álamo. Computing turbulent channels at experimental Reynolds numbers. In M. Behnia, W. Lin, and G. D. McBain, editors, *Proceedings of the Fifteenth Australasian Fluid Mechanics Conference*, 2004.
- ¹⁵ J. Jiménez, J. C. del Álamo, and O. Flores. The large-scale dynamics of near-wall turbulence. *J. Fluid Mech.*, 505:179–199, 2004.
- ¹⁶ K. C. Kim and R. Adrian. Very large-scale motion in the outer layer. *Phys. Fluids*, 11:417–422, 1999.

- ¹⁷ I. Marusic and N. Hutchins. Experimental study of wall turbulence: Implications for control. In M. Gad el Hak, editor, *Workshop on Transition and Turbulence Control, Singapore, 8-10 December 2004*. 2005.
- ¹⁸ I. Marusic and G. J. Kunkel. Streamwise turbulence intensity formulation for flat-plate boundary layers. *Phys. Fluids*, 15:2461–2464, 2003.
- ¹⁹ I. R. Mclean. *The near-wall eddy structure in an equilibrium turbulent boundary layer*. PhD thesis, University of Southern California, USA, 1990.
- ²⁰ M. M. Metzger and J. C. Klewicki. A comparative study of near-wall turbulence in high and low reynolds number boundary layers. *Phys. Fluids*, 13, 2001.
- ²¹ C. D. Tomkins and R. J. Adrian. Spanwise structure and scale growth in turbulent boundary layers. *J. Fluid Mech.*, 490:37–74, 2003.
- ²² C. E. Wark, A. M. Naguib, and S. K. Robinson. Scaling of spanwise length scales in a turbulent boundary layer. *AIAA-paper*, 91-0235, 1991. 29th Aerospace Sciences Meeting, Nevada.